Soil Biology & Biochemistry 68 (2014) 20–30

Contents lists available at ScienceDirect

Soil Biology & Biochemistry

journal homepage: www.elsevier.com/locate/soilbio

Predicting the effects of biochar on volatile petroleum hydrocarbon biodegradation and emanation from soil: A bacterial community finger-print analysis inferred modelling approach

Paola Meynet [a], Elena Moliterni [c], Russell J. Davenport [a], William T. Sloan [b], José V. Camacho [c], David Werner [a, *]

[a] School of Civil Engineering and Geosciences, Newcastle University, NE1 7RU England, United Kingdom
[b] School of Engineering, University of Glasgow, James Watt South Building, Glasgow G12 8QQ, Scotland, United Kingdom
[c] Chemical Engineering Department, Institute for Chemical and Environmental Technology, Universidad de Castilla La Mancha, 13071 Ciudad Real, Spain

ARTICLE INFO

Article history:
Received 30 January 2013
Received in revised form
9 September 2013
Accepted 10 September 2013
Available online 24 September 2013

Keywords:
Soil remediation
VOCs
Biochar
Soil microbiology
Sorption
Biodegradation

ABSTRACT

We investigated the response of the dominant bacterial taxa in gravelly sand to the addition of biochar and/or mixtures of volatile petroleum hydrocarbons (VPHs) using denaturing gradient gel electrophoresis (DGGE) and sequencing of cut bands. Biochar addition alone had only weak effects on the soil bacterial community composition in batch study samples, while VPH addition had strong effects. Indirect effects of biochar on soil bacterial communities were apparent in column study samples, where biochar-enhanced sorption affected VPH spreading. Following VPH addition, cell abundance increased by no more than a factor of 2 and several *Pseudomonas* spp. became dominant in soil with and without biochar. We present a VPH fate model that considers soil bacterial biomass dynamics and a nutrient limited soil biomass carrying capacity. The model simulates an apparent lag phase before the onset of a brief period of intensive VPH biodegradation and biomass growth, which is followed by substantially slower VPH biodegradation, when nitrogen needs to be recycled between decaying and newly formed biomass. If biomass growth is limited by a factor other than the organic pollutant bioavailability, biochar amendment may enhance VPH attenuation in between a VPH source below ground and the atmosphere by reducing the risk of overloading the soil's biodegradation capacity.

1. Introduction

Biomass-derived charred materials, so-called biochars, have attracted significant research interest due to their carbon storage and climate change mitigation potential (Lehmann, 2007). Charred carbonaceous matter is more resilient to microbial degradation than other forms of organic matter, and adding biochars to soils may lastingly store CO_2 captured from the atmosphere in the terrestrial environment (Zimmerman, 2010). The use of biochar as an amendment for the remediation of contaminated soil (Beesley et al., 2010) offers benefits in addition to those of storing CO_2 captured from the atmosphere. The application of biochars as sorbents for soil remediation is motivated by the successful use of coal-derived activated charcoals for the in-situ sequestration of hydrophobic organic compounds (HOCs) (Ghosh et al., 2011). Activated or non-activated charcoals were shown to reduce hydrophobic organic pollutant leaching (Hale et al., 2012), pollutant loss to the atmosphere (Bushnaf et al., 2011), and uptake from soil by plants (Hilber et al., 2009; Jakob et al., 2012; Vasilyeva et al., 2010), and earthworms (Fagervold et al., 2010; Jakob et al., 2012; Langlois et al., 2011). Replacing coal-derived charcoal in soil remediation applications with biochar would improve the sustainability of remediation efforts by combining the benefits of HOC risk reduction and carbon capture and storage, and also by reducing economic costs (Sparrevik et al., 2011).

One of the concerns regarding the use of biochar for soil remediation is its long-term impact on the persistence of biodegradable pollutants (Rhodes et al., 2008). Hydrophobic organic compounds (HOCs) are strongly bound in microporous domains of charred materials and become unavailable for uptake by soil organisms and plants (Ehlers and Luthy, 2003). This occlusion reduces HOC ecotoxicity, but also hinders HOC accessibility for intracellular biodegradation by soil microorganisms.

We recently reported physicochemical results from laboratory column experiments with mixtures of volatile petroleum

* Corresponding author.
E-mail address: david.werner@ncl.ac.uk (D. Werner).

0038-0717/$ – see front matter © 2013 Elsevier Ltd. All rights reserved.
http://dx.doi.org/10.1016/j.soilbio.2013.09.015

hydrocarbon (VPH) vapours migrating through gravelly sand with and without 2% w/w biochar amendment (Bushnaf et al., 2011). Similar CO_2 fluxes emanating from soil columns with and without biochar indicated a comparable overall extent of VPH biodegradation, while the emanating VPH flux was substantially lower from the biochar amended soil over the 30 day duration of the experiments. The preferential binding and reduced mobility and bioavailability of monoaromatic hydrocarbons apparently resulted in greater biodegradation of more mobile cyclic and branched alkanes in biochar amended soil. A pollutant fate model based on first-order rate biodegradation kinetics of VPHs dissolved in soil porewater was unable to reproduce the characteristics of these measurements (Bushnaf et al., 2011). First-order rate biodegradation kinetic models neglect the dynamics of microbial populations, and this may explain the inaccurate model predictions. We therefore decided to complement the physicochemical observations reported in the previous paper with an investigation of the bacterial community response in gravelly sand with and without biochar to the presence of VPHs and to use the insights gained from both, physicochemical and microbiological measurements, to develop an improved mathematical model for predicting biochar effects on the VPH fate in soil. Our aim was to develop a modelling framework which not only considers biochar effects on the pollutant bioaccessibility and mobility, but also implications for the growth of pollutant degrading biomass together with additional, soil-type specific constraints on the soil biomass carrying capacity. In this paper, we demonstrate model calibration procedures and validate model predictions for gravelly sand and VPHs as a first case study using concepts which may be readily adapted to other soil types, pollutants and biochars.

2. Methods

2.1. Column experiments

The set-up of the column experiments and their chemical data comprising VPH and CO_2 measurements by GC–FID and GC–MS at various sampling locations have been reported by Bushnaf et al. (2011). Briefly, two vertical columns made of glass were homogeneously packed over a length of 43 cm with gravelly sand (water content 10% wet weight, 25% dry weight fine gravel with 2–4 mm particle size, 73.8% dry weight sand with >63 μm particle size, 1.2% silt and clay with <63 μm particle size) with and without 2% dry weight biochar amendment (obtained from Environmental Power International, Wiltshire, UK, made from wood-chips by fast pyrolysis at 800 °C, and added as 2% of soil dry weight). The experimental set-up is illustrated in Fig. 1. The packed columns were left undisturbed for 5 days to monitor the background respiration, which was minimal. After that period, nominally on day 0, a vial containing 10 ml of the VPH mixture was connected to the bottom of the funnel-shaped lower end of the columns and VPH migration was monitored at four sampling ports for 13 days with an open column top. The VPH mixture sources were removed on day 13 and replaced with fresh ones on day 15. The columns were monitored for a further 15 days with an inverted glass beaker placed over the top of the columns, which left a small gap between beaker and column, in order to quantify the emanating fluxes of VPHs and CO_2. Oxygen levels indicated that the soil in the columns remained aerobic for either one of the upper boundary conditions (with and without beaker). After the 30 day monitoring period, two replicate soil samples were taken from the location of each sampling port of the two columns (see Fig. 1) and stored at −20 °C in filter-sterilized phosphate buffer saline (PBS, Oxoid) or in solution 1:1 v/v absolute ethanol: filter-sterilized PBS for the microbial analysis reported in this paper. To evaluate changes of the microbial community during the length of the experiment, two replicate samples of the soil used to pack the columns (initial soil, IS, and initial soil with biochar, ISB) were also stored at −20 °C (in PBS or in solution 1:1 v/v absolute ethanol:PBS) and used as reference samples in the microbial analysis.

2.2. Batch experiments

In this work, additional batches with the soil and biochar employed in the previously reported column experiments were set up. The main purpose of these additional batch studies was to also evaluate the eventual effects of biochar only (i.e. in the absence of VPHs) on bacterial community structure and functioning.

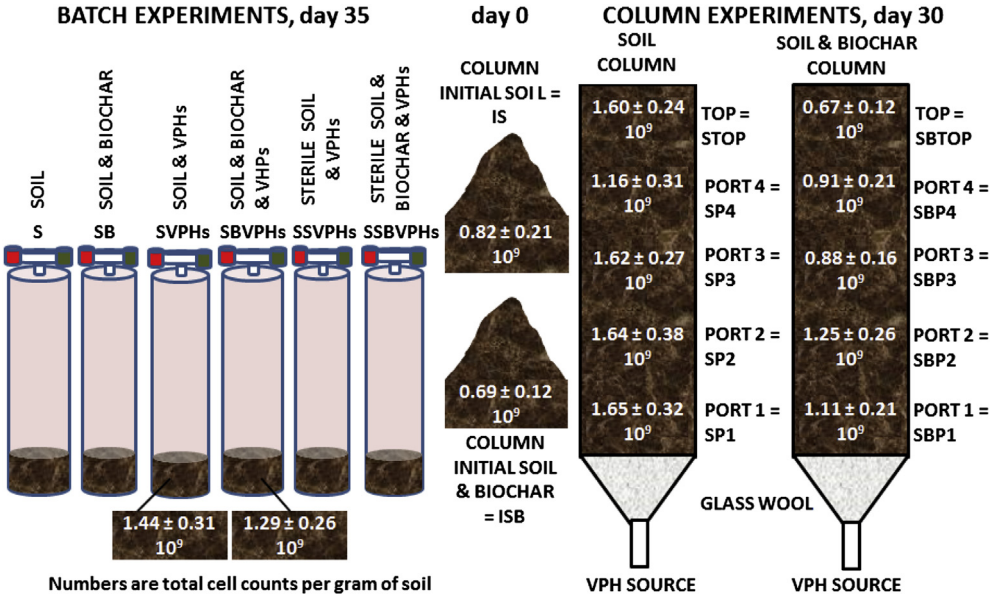

Fig. 1. Illustration of experimental set ups and total cell count results. The errors in the cell counts indicate one standard deviation above and below the calculated mean, based on the results obtained from two different soil samples. For each sample, cell abundance was calculated by direct count of 20 fields of view.

Microcosm batches (live batches) were set up in 65 ml amber vials (Jencons, a VWR Division, Leicestershire, UK) closed with Teflon Mininert valves (Supelco, Bellefonte, USA), each containing 15 g of wet soil only (set-up S, Fig. 1), with addition of 2% soil dry weight biochar (set-up SB, Fig. 1), with addition of 0.03 ml mixture of VPHs (set-up SVPHs, Fig. 1), and with addition of 2% soil dry weight biochar and 0.03 ml VPH mixture (set-up SBVPHs, Fig. 1). A series of sterile batches were run in parallel and they were composed by 15 g of autoclaved soil (121 °C, 30 min) with addition of 0.03 ml VPH mixture (set-up SSVPHs, Fig. 1), and 2% soil dry weight biochar and 0.03 ml VPH mixture (set-up SSBVPHs, Fig. 1). The VPH mixture was composed of 12 major constituents of gasoline or kerosene as described in Bushnaf et al. (2011). The VPH mixture was added to the microcosms by syringing, through the Teflon Mininert valve, 0.03 ml of the mixture into the centre of the soil/biochar and homogenised by thoroughly mixing on an orbital shaker, prior the starting of the experiment. All the treatments and controls were set up in triplicate for the sacrificial solvent extraction of NAPL residuals on day 24 and an additional identical set of triplicate batches was set up for microbial analysis on day 35. The head-space gas from each microcosm was regularly sampled in order to monitor the CO_2 production, as indicator of the microbial activity in the decomposition of VPHs. CO_2 content was measured by gas chromatography–mass spectrometry (GC–MS) (Bushnaf et al., 2011). The chemical data obtained for different treatments were statistically evaluated by the paired *t*-test or one-way ANOVA, using Minitab® 16.1.0 software. On day 35 batch soil samples were split in two for microbial analysis, and frozen at −20 °C with the addition of filtered-sterilized PBS and of an equal volume of a 1:1 (v:v) absolute ethanol: filter-sterilized PBS solution, respectively.

2.3. Molecular analysis

Total cell counts followed the method described in Meynet et al. (2012). Denaturing gradient gel electrophoresis (DGGE) was carried out to determine similarities and differences between the predominant bacterial communities in the experimental treatments, and to identify selected members of these communities. Total bacterial DNA was extracted from 0.5 g (wet weight) aliquots of the stored (without ethanol) soil samples using Fast DNA Soil Kit (Qbiogene). Primers 2 and 3 (Muyzer et al., 1993), targeting the Bacteria, were used to PCR amplify the V3 region of bacterial 16S rRNA gene fragments, and the PCR products were analyzed by DGGE as described by Hale et al. (2010). Where possible within the maximum numbers of lanes per gel, the PCR products were run twice on the same gel, to show the reproducibility of the band pattern. The DGGE images were normalized and interpreted using the image analysis software BioNumerics (Applied Maths NV, St. Martens-Latem, Belgium). Primer 6 software (Primer-E Ltd., Plymouth, UK) was used to perform cluster analysis using the Pearson product–moment correlation coefficient followed by Analysis of Similarity (ANOSIM).

Sixteen DGGE bands were excised from the batch study gel and 50 bands from the column study gel, PCR-amplified using primers 2 and 3, purified and sequenced as previously described (Hale et al., 2010). Sequences were compared against the Ribosomal Database Project (RDP10) and GenBank databases using the BLAST algorithm to determine the closest matching sequence identity.

2.4. Model

In the previous paper we concluded that the characteristics of the measured break-through curves were not well reproduced by model simulations based on first-order biodegradation kinetics (Bushnaf et al., 2011). We therefore propose an alternative model of VPH biodegradation, which considers growth of VPH degrading biomass in conjuncture with growth limiting factors such as VPH and inorganic nutrient availability. In this new model, the partial differential equation describing the mass balance for VPH compound *k* at vertical location *z* (cm) within the soil filled column and at time *t* (s) is still given by:

$$\left(\theta_a + \frac{\theta_w}{H_k} + \frac{\rho_s \theta_s K_{d,k}}{H_k} + \frac{\rho_{bc}\theta_{bc}K_{bc,k}}{H_k}\right)\cdot\frac{\mathrm{d}}{\mathrm{d}t}C_{a,k}(z,t) = \theta_a \tau_a D_{a,k}\cdot\frac{\partial^2}{\partial z^2}C_{a,k}(z,t) - \theta_w \cdot r_{w,k} \quad (1)$$

where $C_{a,k}$ (g/cm^3) is the concentration of compound *k* in soil pore-air, τ_a (−) is the tortuosity factor, θ_a (−), θ_w (−), θ_s (−), and θ_{bc} (−) are the air, water, soil particle and biochar particle filled volume fractions of the soil, ρ_s (g/cm^3) and ρ_{bc} (g/cm^3) are the densities of soil and biochar particles, H_k (−) is the dimensionless Henry's constant of compound *k*, $K_{d,k}$ (cm^3/g) and $K_{bc,k}$ (cm^3/g) are the particle–water partitioning coefficients of compound *k* for soil and biochar particles respectively, $D_{a,k}$ (cm^2/s) is the molecular diffusion coefficient of compound *k* in air, and $r_{w,k}$ (g/cm^{3}s) is the compound *k* removal rate from the soil water phase, i.e. we assume that only the water-dissolved fraction of the VPH mass is available for biodegradation. This assumption is in line with mass transfer limited pollutant biodegradation often observed in soil (Harms and Bosma, 1997), although some bacteria may be able to also degrade sorbed compounds (Yang et al., 2009).

After an initial lag phase during which $r_{w,k}$ (g/cm^{3}s) is zero, the VPH compound removal rate $r_{w,k}$ is defined by:

$$r_{w,k} = k_{\mathrm{deg},k}\cdot\frac{1}{Y_k}\cdot\frac{C_{a,k}(z,t)}{H_k}\cdot C_{w,n}(z,t)\cdot C_{w,b,\mathrm{VPH}}(z,t) \quad (2)$$

where $k_{\mathrm{deg},k}$ (cm^6/(g N g VPH s)) is a third order growth rate, Y_k (g biomass C/g VPH) is the biomass yield coefficient for compound *k*, $C_{w,n}$ (g N/cm^3) is the concentration of a critical growth factor in soil porewater, which we assume to be inorganic nitrogen, and $C_{w,b,\mathrm{VPH}}$ (g biomass C/cm^3) is the VPH degrading biomass concentration in soil porewater. This rate expression can be interpreted as a factored Monod kinetics model for the case in which inorganic nutrient and VPH substrate concentrations are both below their respective "half-maximum rate" concentrations.

Change in the VPH degrading biomass, $C_{w,b,\mathrm{VPH}}$ (g of biomass C/cm^3), is described by:

$$\frac{\mathrm{d}}{\mathrm{d}t}C_{w,b,\ \mathrm{VPH}}(z,t) = \left[\left(\sum_k k_{\mathrm{deg},k}\cdot\frac{C_{a,k}(z,t)}{H_k}\cdot C_{w,n}(z,t)\right) - d\right]\cdot C_{w,b,\mathrm{VPH}}(z,t) \quad (3)$$

where *d* (1/s) is the decay rate of the VPH degrading biomass. For the rest of the initial biomass $C_{w,b,\mathrm{non\ VPH}}$ (g of biomass C/cm^3), we assume that it decays with the same rate, while its growth is negligible.

$$\frac{\mathrm{d}}{\mathrm{d}t}C_{w,b,\mathrm{non\ VPH}}(z,t) = -\mathrm{d}\cdot C_{w,b,\mathrm{non\ VPH}}(z,t) \quad (4)$$

If we assume, that *f* (g N/g biomass C) is the elemental fraction of nitrogen relative to carbon in biomass, the change in the readily available nitrogen concentration in soil porewater due to biomass growth and decay is described by:

$$\frac{\mathrm{d}}{\mathrm{d}t}C_{w,n}(z,t) = -f\cdot\left[\left(\sum_k k_{\mathrm{deg},k}\cdot\frac{C_{a,k}(z,t)}{H_k}\cdot C_{w,n}(z,t)\right) - d\right] \cdot C_{w,b,\mathrm{VPH}}(z,t) + f\cdot d\cdot C_{w,b,\mathrm{non\ VPH}}(z,t) \quad (5)$$

The lower boundary condition of the column study is implemented by calculating VPH concentrations in air in equilibrium with the liquid VPH mixture in the source using Raoult's law. The source composition is recalculated at each time step based on the VPH loss caused by the gas-phase vapour diffusion across the tubular section in the lowermost part of the column connected to the source (see Fig. 1). The diffusive VPH mass flux across this section is set equal to the diffusive VPH mass flux at the bottom of the soil-filled column volume to account for the column geometry. The source is removed on day 13 and replace with a fresh source on day 15. For the first 15 days with the open column top a zero concentration boundary condition is implemented at the top of the soil-filled column volume. From day 15 onwards a zero concentration boundary condition is implemented at the end of the gap between the column and the inverted beaker placed on top of the column, and the diffusive VPH mass flux through the beaker gap is set equal to the flux at the top of the soil-filled column volume.

2.5. Model assumptions

In addition to a number of simplifying physicochemical assumptions, already described in Bushnaf et al. (2011), the improved modelling approach makes the following simplifying assumptions regarding VPH biodegradation: The activities of all the VPH degrading microorganisms are represented by one kind of VPH degrading biomass with a constant elemental composition, compound-specific removal rate and compound-specific yield. This VPH degrading biomass may for instance consist of microorganisms initiating the biotransformation of VPHs and microorganisms growing on the metabolites of this initial transformation, with the yield representing the average amount of VPH degrading biomass formed per mass of VPH compound transformed into VPH degrading biomass and CO_2 by this mixed heterotrophic microbial community. We assume a constant biomass decay rate for VPH degrading and non-VPH degrading biomass and neglect growth on carbon substrates other than VPHs and their metabolites. We assume a fixed amount of nitrogen in the system comprised of the initial water extractable inorganic nitrogen and the estimated initial biomass nitrogen, and thereby ignore the high complexity of microbial nitrogen cycling in soils. We also assume that the elemental nitrogen released from decaying biomass becomes immediately available for new biomass formation. We make these assumptions to obtain a VPH fate model which can be calibrated using available experimental data, and some literature data, in order to forward predict VPH concentrations at various sampling locations in the column study, which can then be compared with independently measured experimental data. If we were, for example, to represent specific interactions of 20 distinct microbial taxa with 12 VPH compounds the number of model parameters $k_{\mathrm{deg},k}$ alone would increase from 12 in the current model to 240, far higher than the number of parameters values which can be derived from the available data.

3. Results and discussion

3.1. Chemical results batch study

The chemical measurements of the batch study are in line with earlier results (Bushnaf et al., 2011), and are described in more detail in Supporting information. Briefly, following VPHs addition, soil respiration increased significantly and to a similar extent in soil with and without biochar (Fig. S1a and b). Without VPH addition, batches containing soil with and without biochar produced similar, much lower amounts of CO_2, indicating that more than 90% of the CO_2 produced following VPH addition can be attributed to VPH biodegradation (Fig. S1a and b). Contrary to other reports (Luo et al., 2011), we observed no temporary stimulation of soil respiration through biochar addition alone. Therefore, VPHs are the main carbon substrates considered for modelling microbial growth in this gravelly sand (Eqs. 2–4).

Amounts of VPHs extracted from the batches on day 24 were high for most compounds (Fig. S1c), indicating only limited VPH biodegradation. For toluene, a 13% difference in the residual amounts between soil with and without biochar was statistically significant (t-test, $p = 0.02$), and can be explained by particularly enhanced toluene sorption (Bushnaf et al., 2011) and therefore reduced toluene bioavailability in the biochar amended soil. For all the other compounds, VPH residuals were comparable in soil with and without biochar (SVPHs vs. SBVPHs, t-test, $p > 0.2$ for all compounds).

3.2. Total cell counts

Total cell count was used to estimate the increase and spatial variability in bacterial cell abundance in the soil samples from column experiments following VPH addition. In the columns, cells numbers significantly increased from the cell counts of the initial soil samples (IS and ISB) in both treatments (t-test, $p < 0.01$ for IS/ISB vs average of all ports in soil/biochar column), which lends support to our presumption that biomass growth needs to be considered for modelling the VPH fate in the columns. Higher variability in cell numbers was measured across the column with biochar (one-way ANOVA, $p < 0.001$), while cell numbers were more uniform in the one without biochar, with exception of port 4 (STOP, SP3, SP2, SP1, one-way ANOVA, $p = 0.766$; group STOP, SP3, SP2, SP1 vs SP4, t-test $p < 0.001$). Total cell counts in the column study increased by no more than a factor of about 2 following VPH addition over a one month period, indicating a limited biomass carrying capacity of the soil (Fig. 1). For comparison, cells were also counted at the end of the batch study for the live soil samples with VPH addition (SVPHs, SBVPHs) and these counts were also broadly comparable with those in samples taken at the end of the column study.

Inorganic nitrogen availability is likely limiting microbial growth following VPH addition. The soil initially contained <1 μg/g d.w. nitrate and nitrite nitrogen and 6.7 ± 0.3 μg/g d.w. ammonia nitrogen or between 6.7 and 7.7 μg/g readily available inorganic nitrogen in total. Water extractable nutrient contents reported by Bushnaf et al. (2011) show that addition of 2% w/w biochar adds only 0.01 μg/g d.w. readily available nitrate and nitrite nitrogen and 0.03 μg/g d.w. ammonia nitrogen, and therefore does not significantly enhance the amended soil nitrogen availability. Based on a biomass nitrogen to carbon ratio of 1:10 (in the middle of the range reported by Bamforth and Singleton (2005)) and 100 fg of biomass carbon per soil bacterial cell (Whitman et al., 1998), the water extractable inorganic nitrogen in the soil would allow for the build-up of between 6.7 and $7.7^{*}10^{8}$ new cells per g of soil which agrees approximately with the maximum observed increases in the total cell count of $8.3^{*}10^{8}$ new cells observed in the lower part of the soil column without biochar. This suggests that the soil biomass carrying capacity can be roughly predicted based on the readily available inorganic nitrogen. We consider this limitation in Eq. (3) of our improved pollutant fate model, where the growth rate becomes negligible when the inorganic nitrogen concentration in soil porewater drops towards zero.

3.3. Changes in the predominant bacterial community structures

Distinct bacterial communities were observed in the different treatments from the batch study (Fig. 2a). The initial pure biochar samples (IB) yielded few quantifiable DGGE gel bands indicating a low bacterial content. DNA extracted from autoclaved soil with and without biochar, and in either case with VPH addition, yielded a few weak bands in their respective DGGE lanes (SSVPHs and SSBVPHs), which indicates some re-growth of bacteria, possibly from spores, although autoclaved soil respiration following VPH addition remained far below live soil respiration (Fig. S1a in supporting information). Distinct bacterial communities were also observed for the column experiment with and without biochar (Fig. 2b), with variation in different operational taxonomic unit (OTU) abundances (i.e. DGGE band intensities) at the different sampling ports. In both batch and column studies, the bacterial communities from duplicate samples of identical treatments showed high similarity based on cluster analysis of Pearson product–moment correlation coefficients, demonstrating good method reproducibility (Fig. 2c and d). Differences in bacterial community structure in the cluster analysis mapped neatly onto treatments.

One-way ANOSIM of the day 35 samples confirmed VPH addition as a significant factor in determining shifts in bacterial community structure in the batch study ($R = 1$, $p = 0.03$), whereas biochar was not a statistically significant factor ($R = 0.198$, $p = 0.17$). Without addition of VPHs the predominant bacterial community structure shifted more strongly with time than in response to biochar amendment, which is in line with our earlier field observation of only minor effects of activated charcoal on bacterial community structure in an urban soil (Meynet et al., 2012). The properties of the biochar and soil used in this study may explain why the impacts of biochar *per se* were minor: i) the initial soil pH of 7.96 ± 0.04 was already alkaline and not measurably increased by 2% biochar addition (Bushnaf et al., 2011); ii) 2% biochar addition did not significantly alter the water soluble nitrogen content of the soil, because nitrogen tends to volatilize in high temperature

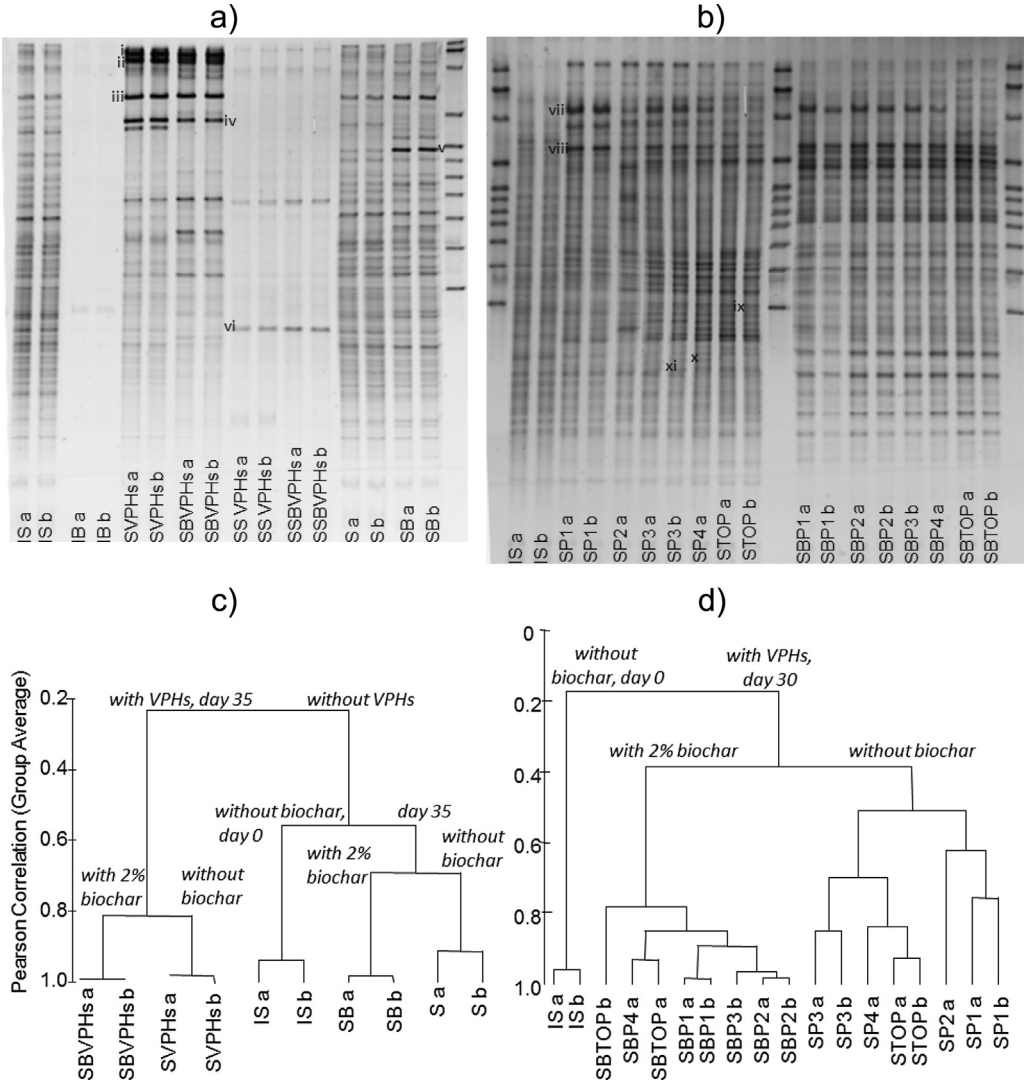

Fig. 2. DGGE gel image from a) the batch study and b) the column study with the location of sequenced bands having >98% similarity matches in the GenBank databases: i) *Pseudomonas abietaniphila* strain 99; ii) *Pseudomonas putida* strain J-18; iii) Pseudomonas *putida* strain DE5; iv) *Pseudoxanthomonas* sp. C2603; v) Uncultured proteobacterium clone APC_4_B10; vi) Uncultured bacterium clone BLAM-OTU14; vii) *Pseudomonas* sp. NBRC 101724; viii) *Pseudomonas* sp. DCY73; ix) Uncultured soil bacterium clone B14-4; x) Uncultured *Rhodococcus* sp. isolate; xi) Uncultured bacterium clone Upland_8_4652. Also shown is a cluster analysis of bacterial communities using Pearson product–moment correlation coefficients of relative band intensity patterns for c) the batch study and d) the column study. A key to labels on the lanes is presented in Fig. 1. Additional band sequencing data is provided as Supporting information.

pyrolysis, and wood derived biochars tend to have lower nitrogen contents than biochars made from other source materials (Novak et al., 2012); iii) soil texture effects of biochar (Atkinson et al., 2010), such as improved aeration, were likely small in gravelly sand; iv) high pyrolysis temperature biochars have low leachable organic carbon contents (Bruun et al., 2011) and tend not to stimulate soil respiration (Luo et al., 2011); v) biochar effects on water retention (Jeffery et al., 2011) were not relevant in our enclosed experiments; vi) the biochar used in this study did not contain a significant amount of native bacteria which could have added new members to the predominant soil bacterial community (Fig. 2a).

ANOSIM of day 30 samples from the column study confirmed biochar as a significant factor determining the bacterial community structure in the column experiments ($R = 0.89$, $p = 0.001$). Additional differences in bacterial community structure within the respective biochar treatments are formed based on distance from the VPH source at the bottom of the columns (Fig. 2d). In the column experiments, biochar-enhanced sorption of VPHs not only affected the local solid–water–air partitioning of, in particular, monoaromatic hydrocarbons, but also their vapour-phase migration and thereby spatial distribution within the columns. These results suggest that the main biochar effect on soil bacteria is indirect – through its sorption of VPHs, which are much better growth substrates than biochar, and implications for VPH spreading and availability for biodegradation. Biochar effects on VPH sorption and mobility in soil were incorporated in the model through the definition of an additional sorbent matrix with VPH compound-specific biochar-water distribution coefficients, K_{bc} (see Eq. (1)).

The relative DGGE band intensities were used as a proxy for the relative operational taxonomic unit (OTU) abundance, which are compared in ranked order in Fig. 3. The steepness of the slope can be used as indicator for dominance or evenness in the taxa abundance distribution. Fig. 3 shows that the evenness of the soil bacterial community decreases in response to VPH addition, in particular in the batch study, which suggests that VPHs benefit some taxa at the expense of other taxa, which decrease in relative abundance. The model partially accounts for these changes in the microbial community composition by distinguishing the VPH degrading biomass, $C_{w,b,\mathrm{VPHs}}$, which increases in relative abundance following VPH addition, from the rest of the initial biomass, $C_{w,b,\mathrm{non\ VPHs}}$, which decays and decreases in relative abundance (see Eqs. 3 and 4).

In the batch study, only one of the 40 most abundant OTUs was unique to biochar amended soil (with and without VPH addition) and only one was unique to soils with VPH addition (with and without biochar addition, Fig. 3a and b). Three quarters of the 40 most abundant OTUs in VPH exposed soil samples with and without biochar from the column study were also predominant members of the original bacterial community, only one of the 40 most abundant OTUs is specific to the soil column with biochar, and only three of the 40 most abundant OTUs are specific to the soil column without biochar. This suggests that a substantial portion of the VPH degrading OTUs is already predominantly present in the original soil bacterial community.

3.4. Identification of OTUs

Closest matching sequence identities in the BLAST search and RDP classification results for sixteen bands cut from the batch DGGE gel and fifty bands cut from the column DGGE gel are presented as supporting information in Figs. S2 and S3 and Tables S1 and S2. Their phyla association is also shown in ranked order in Fig. 3. An apparent trend in particular following VPH addition is the upwards movement in the ranking of bands classified as Proteobacteria (labelled P in Fig. 3) at the expense of bands classified as belonging to the Gram-positive phyla of Actinobacteria and Firmicutes (labelled A and F in Fig. 3), some members of which are known to form spores. High BLAST-search sequence similarity matches with *Pseudomonas* spp. were obtained for several DGGE band sequences with high relative intensity and OTU ranking in VPH treated soils (bands i–iv, vii, viii in Fig. 2a and b). Some of these DGGE bands (i, ii, iii, viii) were already predominantly present in the initial soil samples, while others (iv, vii) were not. Members of the genus *Pseudomonas* are well-known, versatile utilizers of petroleum hydrocarbons, including linear (Dinamarca et al., 2002), cyclic (Anderson et al., 1980) and monoaromatic compounds (Assinder and Williams, 1990), and tend to increase in abundance at petroleum spill sites (Margesin et al., 2003). These soil bacteria were indigenous, since we did not inoculate the soil. The investigated gravelly sand did not have a measureable VPH content or known VPH exposure history, but catabolic capability to degrade VPHs is common in the soil environment (Elazhari-Ali et al., 2013; Kjeldsen et al., 2003; Pasteris et al., 2002).

3.5. Estimated biodegradation model parameters

The initial total biomass concentration in g biomass C per cm^3 of soil pore-water and initial readily available inorganic nitrogen concentration in g N per cm^3 of soil pore-water was calculated from the total cell count, water-extractable inorganic nitrogen measurements and water content of the initial soil and an assumed carbon content of 100 fg of biomass carbon per soil bacterial cell (Whitman et al., 1998). For further model calibration, we estimated absolute OTU abundances by multiplying relative OTU abundances shown in Fig. 3 with the respective total cell counts. This estimation ignores the fact that DGGE relative band intensity is only an indication of relative OTU abundance, and DGGE captures only the predominant soil bacterial community, whereas the total cell counts also includes rare OTUs not detected by DGGE. Predominant OTUs probably contribute the majority of the total cell count since bacterial communities are often log-normally distributed (Curtis et al., 2002), lending validity to our simplified estimates of absolute OTU abundances. To distinguish between $C_{w,b,\mathrm{VPH}}(0)$ (VPH degraders in the initial biomass) and $C_{w,b,\mathrm{non\ VPH}}(0)$ (rest of the initial biomass), we compared estimated OTU abundances before and after VPH addition. OTUs which showed on average an abundance increase following VPH addition were attributed to the VPH degrading biomass $C_{w,b,\mathrm{VPH}}(0)$, and the rest of the OTUs where considered to belong to $C_{w,b,\mathrm{non\ VPH}}(0)$. It was thus roughly estimated that between 45% (estimated based on OTU abundance at the end of the biochar amended soil column study) and 53% (estimated based on OTU abundance at the end of soil column study) of the biomass in the initial column study soil sample (ISa and ISb in Fig. 2b) belonged to the VPH degrading biomass.

To estimate an average biomass decay rate, d, we compared the sum of the estimated abundances of non-VPH degrading OTUs, $C_{w,b,\mathrm{non\ VPH}}$, in the initial soil samples and at the end of the column experiments. The average biomass decay rate was then derived from Eq. (4) and found to be $2.5 \cdot 10^{-7}$ (s^{-1}) for the soil without and $5.7 \cdot 10^{-7}$ (s^{-1}) for the soil with biochar. This compares with a decay rate, d, of $3 \cdot 10^{-6}$ (s^{-1}) used by Bauer et al. (2008) in their simulation of petroleum hydrocarbon degradation in aquifer material inoculated with *Pseudomonas putida* strains.

Biomass yield coefficients were calculated based on the carbon content of each VPH compound and an average yield of 0.5 g of biomass carbon per g of petroleum hydrocarbon carbon which was reported by Elazhari-Ali et al. (2013) for sand in which the predominant soil bacterial community was also dominated by *Pseudomonas* spp. following addition of the same 12 VPH compounds. This assumes that the VPH compound specific yield is only

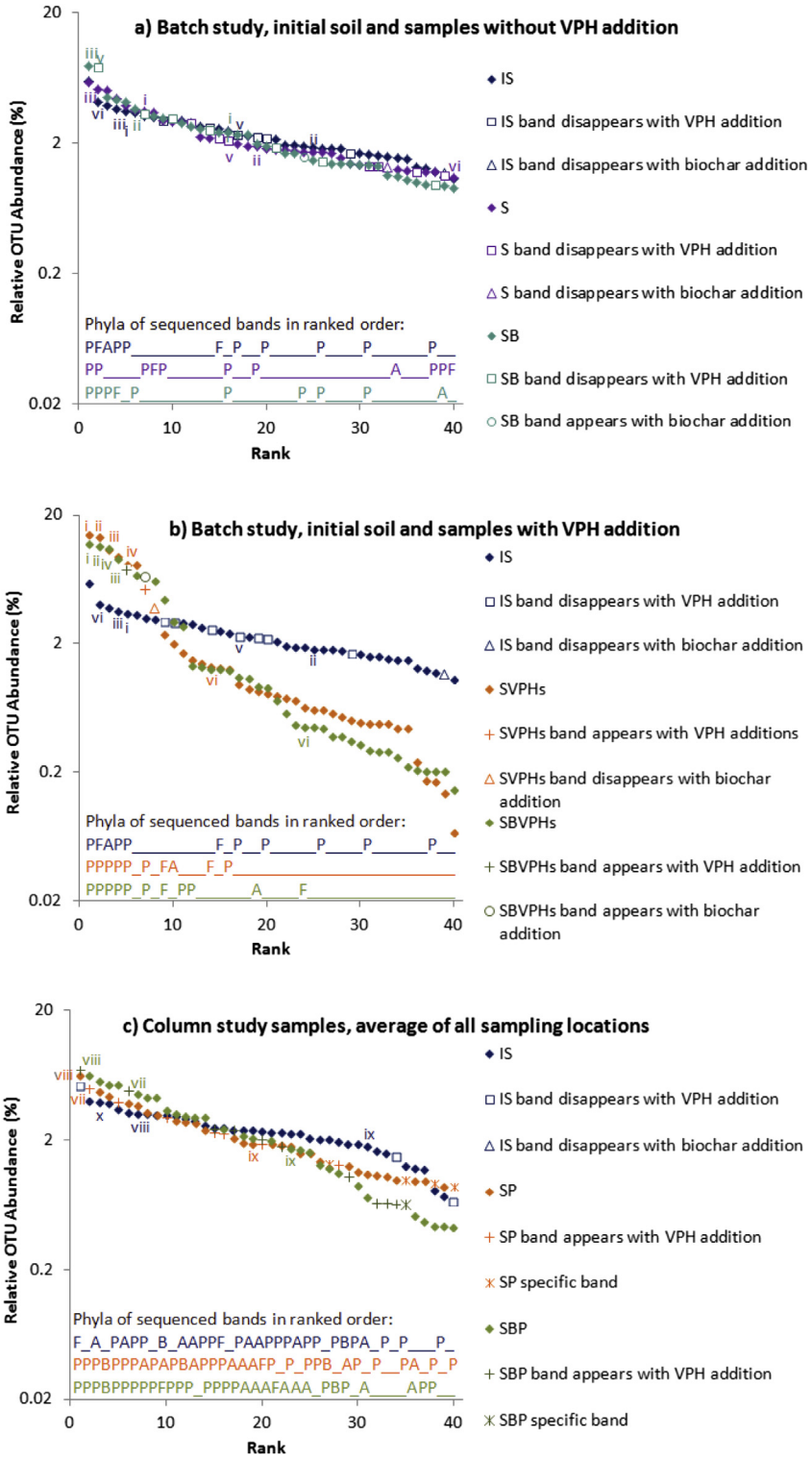

Fig. 3. Relative operational taxonomic unit (OTU) abundance distribution and phyla associations (P = Proteobacteria, B = Bacteroidetes, A = Actinobacteria, F = Firmicutes) of sequenced bands (_ = band not sequenced) in ranked order. The roman numerals correspond to the sequenced bands in Fig. 2. A key to labels on the legend is presented in Fig. 1.

governed by carbon content, which is in line with the observation of a fairly constant ratio of substrate carbon assimilated to total utilized by mixed heterotrophic cultures of soil and sewage sludge bacteria (Payne, 1970).

Compound specific degradation rates, $k_{deg,k}$, were estimated by dividing the first-order rates for VPH degradation in the soil porewater phase, k_w, reported by Bushnaf et al. (2011) for batches exposed to a small amount of VPH vapour by the initial soil VPH degrading biomass concentration, $C_{b,w,VPH}(0)$, and the initial, readily available inorganic nutrient concentration, $C_{n,w}(0)$, and by multiplying with the yield coefficients. In the batch study reported by Bushnaf et al. (2011), headspace concentrations showed that

some VPHs were almost instantaneously degraded, while others were degraded after an apparent lag phase of up to 3 days duration. Since we assumed a composite VPH degrading biomass in our model and neglected substrate–substrate inhibition of VPH biodegradation, we used a mid-range lag phase of 1.5 days before the onset of VPH biodegradation for our model calibration.

3.6. Model results

Predictions of the pollutant fate model are compared with independent measurements at column port 3 (in the middle of the columns), and also in the inverted beaker placed on top of the columns from day 15 onwards to compare the predicted with the measured VPH emanation from soil in the second part of the experiment (Fig. 4). The model predicts an early peak in the VPH breakthrough at port 3 during the initial biodegradation lag phase which is followed by a brief period of intensive VPH biodegradation, causing a temporary dip in the simulated breakthrough curves, especially notable for the most readily biodegradable VPHs such as octane or toluene. During this period, the simulated VPH degrading biomass, $C_{w,b,\mathrm{VPH}}(t)$, grows and uses up the inorganic nitrogen in soil porewater (Fig. S4 in supporting information). Once

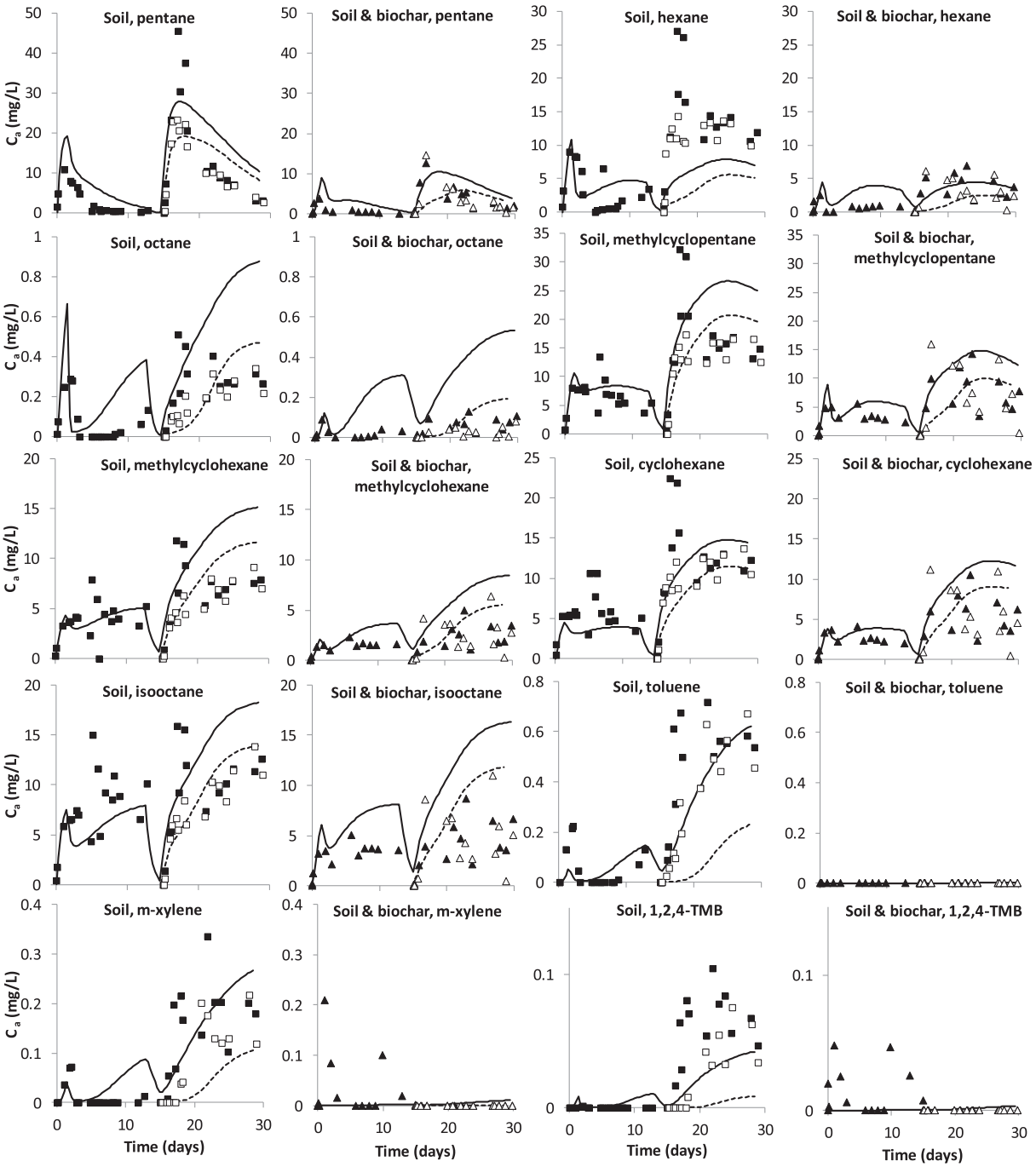

Fig. 4. Measured (symbols) and simulated (lines) VPH breakthrough curves at sampling port 3, which is located in the middle of the soil-filled columns (filled symbols, solid lines), and in the inverted beaker placed on top of the columns from day 15 onwards (empty symbols, broken lines) for soil columns with and without biochar. Simulations are independent predictions without fitting to the experimental data shown in the figure. The NAPL source was removed from the bottom of the columns on day 13 and replace with a fresh NAPL source on day 15. Not shown in the figure are the VPH compounds decane and dodecane for which measured concentrations were mostly below the detection limit.

the inorganic nitrogen in soil porewater has been depleted, further VPH biomass growth in the model simulation relies on recycling nitrogen between decaying and newly formed biomass. As a consequence, the simulated VPH removal is much slower. When the simulated VPH source at the bottom of the columns is removed on day 13 and replaced with a fresh source on day 15, the simulated inorganic nitrogen in soil porewater remains at a very low level (Fig. S4 in supporting information), and hence VPH biodegradation remains slow for the remainder of the simulated experiment. The measured VPH data are broadly in line with these predicted overall trends, and the model anticipates for the soil without biochar breakthrough of readily biodegradable VPHs such as toluene and octane into the column headspace in the second half of the experiments, which was not predicted by the first-order rate model (Bushnaf et al., 2011). The improved model also correctly predicts generally lower VPH concentrations in the soil with biochar as compared to without biochar, even for compounds with high volatility and therefore minimal biochar partitioning (see for example pentane, hexane and methylcyclopentane in Fig. 4). Chromatographic separation of compounds with greater partitioning from pore space air to the biochar (for example toluene) from those with lesser partitioning to biochar (for example pentane) reduces an apparent overloading the bacterial community's VPH removal capacity.

3.7. Sensitivity analysis

A sensitivity analysis shows that the model predictions are fairly robust with regards to changes in the parameter values (i.e. to half the value, Fig. 5) for the lag phase (blue line in Fig. 5) and the initial size of the VPH degrading biomass, $C_{w,b,\mathrm{VPH}}$ (red line in Fig. 5), and the degradation rates, $k_{\mathrm{deg},k}$ (purple line in Fig. 5). These model parameters mainly affect the very early trends in the breakthrough curves, before the simulated VPH biodegradation becomes controlled by the scarce inorganic nitrogen availability. Accordingly, changes in the parameter values for the yield coefficients, Y_k, and the biomass decay rate, d, have greater impacts, because they strongly affect the simulated VPH biodegradation under inorganic nutrient limited conditions. A smaller biomass yield implies that a greater amount of VPH carbon can be biodegraded with a fixed amount of inorganic nitrogen, and consequently halving yield coefficients results in lower predicted VPH concentrations in soil air (green line in Fig. 5). A smaller biomass decay rate implies less nitrogen recycling between decaying and newly formed biomass, and hence less VPH biodegradation and higher VPH concentrations in soil air (orange line in Fig. 5).

3.8. Remaining model short-comings

While the numerical model reproduces the general trends observed in the measured data, there are also some noteworthy discrepancies. The temporary VPH concentration dip at port 3 during the intensive biodegradation phase was longer than predicted by the model (see for instance octane in Fig. 4). A possible explanation could be a delay before soil bacteria reduce their VPH metabolisms in response to the greater scarcity of inorganic nitrogen in soil porewater. Also, the biodegradation of monoaromatic hydrocarbons (toluene, m-xylene, 1,2,4-TMB) in the soil without biochar may have been overestimated by the numerical simulation during the second half of the experiments. A possible explanation could be that the soil bacterial community had already adapted to the presence of straight-chain alkanes by the time monoaromatic hydrocarbons broke through into the upper part of the soil column without biochar, and was therefore less effective at concurrently removing monoaromatic hydrocarbons as compared to the batch study, in which all twelve VPH compounds were simultaneously present from the beginning. A further discrepancy between simulated and measured data in the biochar amended soil are the measured spikes in m-xylene and 1,2,4-TMB concentrations in the first half of the experiment. These elevated concentrations, which were only measured in the centre of the biochar amended column (i.e. were temporarily higher at sampling port 3 than at sampling port 1 in the lower half of the column), could indicate a local wane in the biodegradation of these two compounds, leading to a temporary release of biochar-sorbed m-xylene and 1,2,4-TMB into air in the middle of the biochar amended soil column. Such deviations between the simulations and measurements are expected to result from the simplifying modelling assumptions regarding the VPH biodegradation. For instance, our soil bacterial community structure analysis suggests that many different taxa are involved in VPH degradation, and the microbial community composition is spatially variable, especially in the soil without biochar (Fig. 2d) whereas the model assumes a composite VPH degrading biomass with consistent attributes through the length of the soil columns. The total cell count (Fig. 1) also suggests more variability in population size than predicted by the model for day 30 of the experiments (Fig. S4 in supporting information). Despite of such short-comings, the model can rationalize important differences in the VPH fate observed in

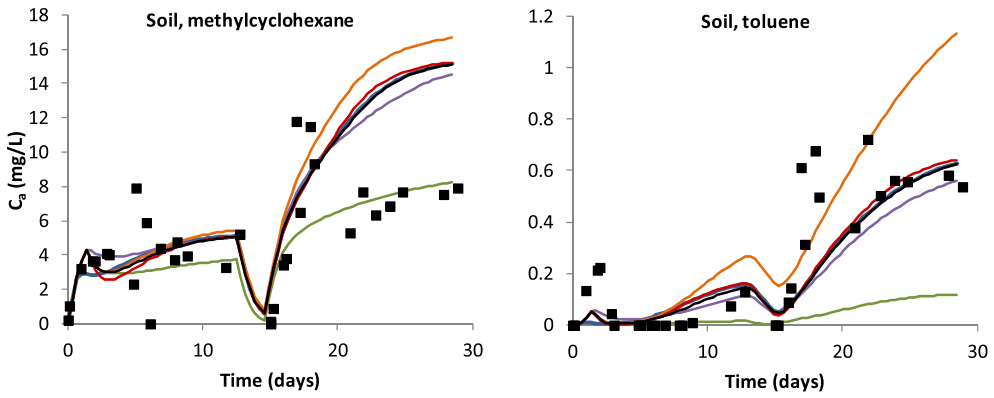

Fig. 5. Sensitivity analysis illustrating the effect of halving the parameter value of the lag phase (blue line), the initial VPH degrading biomass, $C_{w,b,\mathrm{VPH}}(0)$ (red line), all the compound-specific degradation rates, $k_{\mathrm{deg},k}$ (purple line), the biomass decay rate, d (orange line), and all the compound-specific yield coefficients, Y_k (green line), in comparison with the measured breakthrough curves at sampling port 3 (filled square symbols) and the original simulation (black solid line). Methylcyclohexane is shown as an example for a less readily biodegradable VPH compound and toluene as an example for a readily biodegradable VPH compound. (For interpretation of the references to colour in this figure legend, the reader is referred to the web version of this article.)

soil with and without biochar by considering VPH degrading biomass growth, and an inorganic nutrient-limited soil biomass carrying capacity.

4. Conclusions

Our bacterial community finger-printing and modelling analysis shows that, in addition to the compound-specific biochar-enhanced sorption of VPHs and implications for their bioavailability and mobility, microbial population dynamics, in particular biomass yields and decay rates, and soil-type specific population growth limitations are also important for understanding the effects of biochar on the fate of biodegradable pollutants in soil. Chromatographic separation of strongly sorbing from less strongly sorbing compounds during pollutant vapour migration reduces risks of overloading of a soil's pollutant biodegradation capacity. This provides an interesting mechanism by which biochar amendment may in some cases promote instead of hinder the pollution attenuation by biodegradation, and we provide a theoretical framework to model such effects. While other soil types may have higher nitrogen availability than the gravelly sand investigated, other limiting factors will still define a maximum soil biomass carrying capacity, and once this limiting factor has been identified the modelling concept outlined in this paper can be adapted to the site-relevant soil type and pollution scenario. For instance, if near-surface soil above a fluctuating, polluted groundwater table is amended with biochar, the enhanced sorption capacity of this biochar amended soil may prevent rapid breakthrough of volatile organic pollutants occasionally released from a retreating groundwater table (Werner and Höhener, 2002), thus giving soil bacterial communities more time to biodegrade VPHs before they escape to the atmosphere.

Acknowledgements

PM was supported by the Engineering and Physical Research Council (EPSRC) grant EP/F008473/1. RJD would like to acknowledge the Engineering and Physical Research Council (EPSRC) Challenging Engineering funding (EP/I025782/1). We are grateful to the University of Castilla La Mancha that funded EM's visit to Newcastle University. George Mangse assisted with the batch experiments. A sabbatical at the Eberhard Karls University of Tübingen, Germany, supported by the Alexander von Humboldt foundation, enabled DW to develop the numerical model presented in this paper.

Appendix A. Supplementary data

Supplementary data related to this article can be found at http://dx.doi.org/10.1016/j.soilbio.2013.09.015.

References

Anderson, M.S., Hall, R.A., Griffin, M., 1980. Microbial-metabolism of alicyclic hydrocarbons - cyclohexane catabolism by a pure strain of *Pseudomonas* sp. J. Gen. Microbiol. 120, 89–94.

Assinder, S.J., Williams, P.A., 1990. The TOL plasmids – determinants of the catabolism of toluene and the xylenes. Adv. Microb. Physiol. 31, 1–69.

Atkinson, C.J., Fitzgerald, J.D., Hipps, N.A., 2010. Potential mechanisms for achieving agricultural benefits from biochar application to temperate soils: a review. Plant Soil 337, 1–18.

Bamforth, S.M., Singleton, I., 2005. Bioremediation of polycyclic aromatic hydrocarbons: current knowledge and future directions. J. Chem. Technol. Biotechnol. 80, 723–736.

Bauer, R.D., Maloszewski, P., Zhang, Y., Meckenstock, R.U., Griebler, C., 2008. Mixing-controlled biodegradation in a toluene plume – results from two-dimensional laboratory experiments. J. Contam. Hydrol. 96, 150–168.

Beesley, L., Moreno-Jiménez, E., Gomez-Eyles, J.L., 2010. Effects of biochar and greenwaste compost amendments on mobility, bioavailability and toxicity of inorganic and organic contaminants in a multi-element polluted soil. Environ. Pollut. 158, 2282–2287.

Bruun, E.W., Hauggaard-Nielsen, H., Ibrahim, N., Egsgaard, H., Ambus, P., Jensen, P.A., Dam-Johansen, K., 2011. Influence of fast pyrolysis temperature on biochar labile fraction and short-term carbon loss in a loamy soil. Biomass Bioenergy 35, 1182–1189.

Bushnaf, K.M., Puricelli, S., Saponaro, S., Werner, D., 2011. Effect of biochar on the fate of volatile petroleum hydrocarbons in an aerobic sandy soil. J. Contam. Hydrol. 126, 208–215.

Curtis, T.P., Sloan, W.T., Scannell, J.W., 2002. Estimating prokaryotic diversity and its limits. Proc. Natl. Acad. Sci. U. S. A. 99, 10494–10499.

Dinamarca, M.A., Ruiz-Manzano, A., Rojo, F., 2002. Inactivation of cytochrome o ubiquinol oxidase relieves catabolic repression of the *Pseudomonas putida* GPo1 alkane degradation pathway. J. Bacteriol. 184, 3785–3793.

Ehlers, L.J., Luthy, R.G., 2003. Contaminant bioavailability in soil and sediment. Environ. Sci. Technol. 37, 295A–302A.

Elazhari-Ali, A., Singh, A.K., Davenport, R.J., Head, I.M., Werner, D., 2013. Biofuel components change the ecology of bacterial volatile petroleum hydrocarbon degradation in aerobic sandy soil. Environ. Pollut. 173, 125–132.

Fagervold, S.K., Chai, Y.Z., Davis, J.W., Wilken, M., Cornelissen, G., Ghosh, U., 2010. Bioaccumulation of polychlorinated dibenzo-p-dioxins/dibenzofurans in *E. fetida* from floodplain soils and the effect of activated carbon amendment. Environ. Sci. Technol. 44, 5546–5552.

Ghosh, U., Luthy, R.G., Cornelissen, G., Werner, D., Menzie, C.A., 2011. In-situ sorbent amendments: a new direction in contaminated sediment management. Environ. Sci. Technol. 45, 1163–1168.

Hale, S.E., Elmquist, M., Brändli, R., Hartnik, T., Jakob, L., Henriksen, T., Werner, D., Cornelissen, G., 2012. Activated carbon amendment to sequester PAHs in contaminated soil: a lysimeter field trial. Chemosphere 87, 177–184.

Hale, S.E., Meynet, P., Davenport, R.J., Martin Jones, D., Werner, D., 2010. Changes in polycyclic aromatic hydrocarbon availability in River Tyne sediment following bioremediation treatments or activated carbon amendment. Water Res. 44, 4529–4536.

Harms, H., Bosma, T.N.P., 1997. Mass transfer limitation of microbial growth and pollutant degradation. J. Ind. Microbiol. Biotechnol. 18, 97–105.

Hilber, I., Wyss, G.S., Mäder, P., Bucheli, T.D., Meier, I., Vogt, L., Schulin, R., 2009. Influence of activated charcoal amendment to contaminated soil on dieldrin and nutrient uptake by cucumbers. Environ. Pollut. 157, 2224–2230.

Jakob, L., Hartnik, T., Henriksen, T., Elmquist, M., Brändli, R.C., Hale, S.E., Cornelissen, G., 2012. PAH-sequestration capacity of granular and powder activated carbon amendments in soil, and their effects on earthworms and plants. Chemosphere 88, 699–705.

Jeffery, S., Verheijen, F.G.A., van der Velde, M., Bastos, A.C., 2011. A quantitative review of the effects of biochar application to soils on crop productivity using meta-analysis. Agric. Ecosyst. Environ. 144, 175–187.

Kjeldsen, P., Christophersen, M., Broholm, M., Höhener, P., Aravena, R., Hunkeler, D., 2003. Biodegradation of fuel vapours in the vadose zone at Airbase Værløse, Denmark. In: Halm, D., Grathwohl, P. (Eds.), 2nd International Workshop on Groundwater Risk Assessment at Contaminated Sites and Integrated Soil and Water Protection, Tübinger Geowissenschaftliche Arbeiten, vol. 69, pp. 31–39. Tuebingen.

Langlois, V., Rutter, A., Zeeb, B., 2011. Activated carbon immobilizes residual polychlorinated biphenyls in weathered contaminated soil. J. Environ. Qual. 40, 1130–1134.

Lehmann, J., 2007. A handful of carbon. Nature 447, 143–144.

Luo, Y., Durenkamp, M., De Nobili, M., Lin, Q., Brookes, P.C., 2011. Short term soil priming effects and the mineralisation of biochar following its incorporation to soils of different pH. Soil Biol. Biochem. 43, 2304–2314.

Margesin, R., Labbe, D., Schinner, F., Greer, C.W., Whyte, L.G., 2003. Characterization of hydrocarbon-degrading microbial populations in contaminated and pristine alpine soils. Appl. Environ. Microbiol. 69, 3085–3092.

Meynet, P., Hale, S.E., Davenport, R.J., Cornelissen, G., Breedveld, G.D., Werner, D., 2012. Effect of activated carbon amendment on bacterial community structure and functions in a PAH impacted urban soil. Environ. Sci. Technol. 46, 5057–5066.

Muyzer, G., de Waal, E.C., Uitterlinden, A.G., 1993. Profiling of complex microbial populations by denaturing gradient gel electrophoresis analysis of polymerase chain reaction-amplified genes coding for 16S rRNA. Appl. Environ. Microbiol. 59, 695–700.

Novak, J.M., Busscher, W.J., Watts, D.W., Amonette, J.E., Ippolito, J.A., Lima, I.M., Gaskin, J., Das, K.C., Steiner, C., Ahmedna, M., Rehrah, D., Schomberg, H., 2012. Biochars impact on soil-moisture storage in an ultisol and two aridisols. Soil Sci. 177, 310–320.

Pasteris, G., Werner, D., Kaufmann, K., Hohener, P., 2002. Vapor phase transport and biodegradation of volatile fuel compounds in the unsaturated zone: a large scale lysimeter experiment. Environ. Sci. Technol. 36, 30–39.

Payne, W.J., 1970. Energy yield and growth of heterotrophs. Annu. Rev. Microbiol. 24, 17–52.

Rhodes, A.H., Carlin, A., Semple, K.T., 2008. Impact of black carbon in the extraction and mineralization of phenanthrene in soil. Environ. Sci. Technol. 42, 740–745.

Sparrevik, M., Saloranta, T., Cornelissen, G., Eek, E., Fet, A.M., Breedveld, G.D., Linkov, I., 2011. Use of life cycle assessments to evaluate the environmental

footprint of contaminated sediment remediation. Environ. Sci. Technol. 45, 4235–4241.
Vasilyeva, G.K., Strijakova, E.R., Nikolaeva, S.N., Lebedev, A.T., Shea, P.J., 2010. Dynamics of PCB removal and detoxification in historically contaminated soils amended with activated carbon. Environ. Pollut. 158, 770–777.
Werner, D., Höhener, P., 2002. The influence of water table fluctuations on the volatilization of contaminants from groundwater. In: Thornton, S.F., Oswald, S.E. (Eds.), Groundwater Quality: Natural and Enhanced Restoration of Groundwater Pollution, Proceedings of the Groundwater Quality 2001 Conference Held at Sheffield, UK, June 2001. IAHS Publ. No. 275, Sheffield, UK, pp. 213–218.
Whitman, W., Coleman, D., Wiebe, W., 1998. Prokaryotes: the unseen majority. Proc. Natl. Acad. Sci. U. S. A. 95, 6578–6583.
Yang, Y., Hunter, W., Tao, S., Gan, J., 2009. Microbial availability of different forms of phenanthrene in soils. Environ. Sci. Technol. 43, 1852–1857.
Zimmerman, A.R., 2010. Abiotic and microbial oxidation of laboratory-produced black carbon (biochar). Environ. Sci. Technol. 44, 1295–1301.